# On CPM System Design and Simulation

**G. Wade*, M. Fu*, R. Jakobs*, J. Ning*, M. Tomlinson**, and A. Ambroze****

***Abstract*—The various trade-offs in CPM system design are discussed in the context of a realistic system specification. It is shown that power spectra can be adjusted to advantage and that multi-*h* systems are not always beneficial. Accurate system modeling and simulation is vital to design and this is discussed with respect to power spectra, soft decoding, and bit error rate (BER) computation. Straightforward methods for conditional probability determination in soft decoding of CPM, and for noise modeling in BER computation are proposed. Some advanced options for coded CPM are discussed.**

***Index Terms*—decoding, phase modulation, simulation, system modeling.**

## I. INTRODUCTION

THE technology of terrestrial and satellite radio systems is constantly being improved in terms of power and bandwidth efficiency, and a good solution is to employ continuous phase modulation (CPM). Its constant envelope property enables it to be used with non-linear power amplifiers without power back-off, whilst signal bandwidth can be controlled without compromising the constant envelope. Increased power efficiency can be obtained by adding forward error correction (FEC), and this could be combined with the inherent code trellis of CPM to form a turbo-coded system.

CPM system design is a compromise between three factors; power and bandwidth efficiency (reflecting Shannon's capacity formulation), and system complexity. The paper illustrates this using a design example. It also discusses some important aspects of system simulation, such as noise modeling, and the problem of determining probability estimates in soft-decision decoding of CPM.

The essential properties of an *M*CPM signal are expressed in its complex envelope (baseband) form

$$s(t,\underline{a}_n)=\sqrt{\frac{2E_s}{T_s}}\exp[j(f(t,\underline{a}_n)] \;;\; nT_s \le t < (n+1)T_s \qquad (1)$$

$$f(t,\underline{a}_n)=2p\,h\sum_{i=n-L+1}^{n}a_i\,q(t-iT_s)+p\,h\sum_{i=0}^{n-L}a_i \mod 2p \qquad (2)$$

Here, $a_i \in \{\pm 1, \pm 3, \pm 5, \ldots, \pm(M-1)\}$ is a data symbol, $T_s$ is the symbol period, $E_s$ is the symbol energy, and $q(t)$ is the phase response, which is the integral of a frequency pulse $g(t)$ of duration $L$ symbols. Term $\underline{a}_n$ denotes $a_n$ and all previous symbols. Modulation index $h$ is can be defined as $h = 2k/p$, where $k$ and $p$ are relative prime for a finite number of states. The last term in (2) is the phase state, $q_n$, of the CPM trellis, where $q_n \in \{0, 2p/p, 4p/p, \ldots, (p-1)2p/p\}$ i.e. there are $p$ phase states. For $L \ge 2$ the CPM encoder is a finite state machine with state

$$\mathbf{S}_n = (q_n, a_{n-1}, a_{n-2}, \ldots, a_{n-L+1}) \qquad (3)$$

and so the maximum possible number of states in uncoded CPM is $S = pM^{L-1}$ (only $S/2$ states being present in any one symbol period). The number of states, and therefore system complexity, can rapidly become large, and this has led to the development of state-reduction techniques [1][2].

## II. CPM SYSTEM DESIGN

Selection of $M, L, h,$ and $q(t)$ is generally a compromise between bandwidth and power efficiency. For example, decreasing $h$ tends to reduce signal bandwidth, but this also decreases the minimum squared Euclidean distance, $d^2_{\min}$, of the signal, and hence increases the bit error rate (BER) for a specified $E_b/N_0$. Generally speaking, large *L* and *M* tend to give more power and bandwidth efficient systems, but at the expense of increased complexity. Also, sometimes a useful increase in $d^2_{\min}$ can be achieved by using different values of *h* for adjacent symbols (multi-*h*). Parameter selection is further complicated by the trade-off between CPM system complexity and the complexity of any additional FEC. In this case it is necessary to obtain a soft input to the FEC decoder via *a posteriori* probability (APP) decoding of the CPM signal.

### A. Power Spectrum

A typical specification for a 64 kbps CPM system requires the power spectral density (PSD) to be –30 dB at 25 kHz from the carrier, with a BER of $10^{-6}$ at $E_b/N_0 = 12$ dB. The critical normalized frequency is therefore $fT_b \approx 0.4$, where $T_b$ is the bit period. Increasing *L* and the smoothness of $q(t)$ generally improves the spectral response, and here we select $g(t)$ to be the raised-cosine (RC) function. For fixed *h*, the theoretical PSD can be obtained in closed form [3], but a general PSD simulation was also written (in C) in order to handle the multi-*h* case. The simulation uses overlapped Hamming-windowed

This work was supported in part by a Scholarship from the University of Newcastle, NSW, 2308, and by EPSRC grant GR/R14606/01 (UK).

Authors* are with the School of Electrical Engineering and Computer Science, The University of Newcastle, NSW, 2308, and authors** are with the Satellite Centre, University of Plymouth, Devon, UK.

Email: gwade@ee.newcastle.edu.au

ISBN: 1-86467-114-9

data and the usual periodogram averaging. A comparison with theory (Fig.1) shows that simulation is accurate down to at least −50 dB, beyond which simulation deviates from theory due to the Hamming window. Simulation is accurate beyond -70 dB for a Blackman window. Fig. 1 shows that for $M = 4$, 3RC ($L = 3$), $h = 0.25$, the PSD is approximately -32 dB at $fT_b = 0.4$ (a Gaussian function rather than raised cosine gives a virtually identical spectrum). This satisfies the PSD specification. The corresponding number of states is 128, although only 64 are present in any one symbol period due to the time-varying trellis associated with (1) and (2).

The power spectrum can be improved at the specified frequency (25 kHz) by modifying the raised-cosine function. The phase response is defined as

$$q(t) = \int_0^t g(t)\,dt \qquad (4)$$

where $g(t)$ is the RC function. From (2), the instantaneous frequency is

$$\Delta f(t) = \frac{1}{2p}\cdot\frac{d}{dt}j\,(t,\underline{a}_n) = h\sum_i a_i g(t - iT_s) \qquad (5)$$

Since $\Delta f(t)$ depends upon the amplitude of $g(t)$, we could redefine the raised-cosine function as

$$g(t) = \begin{cases} \dfrac{1}{2LT_s}\left(1 - m\cos\dfrac{2p\,t}{LT_s}\right) & ; \quad 0 \le t \le LT_s \\ 0 \quad ; \quad \text{otherwise} \end{cases} \qquad (6)$$

where a factor $m \le 1$ has been introduced into the usual function in order to reduce pulse amplitude. This tends to affect the main spectral lobe, as shown in Fig. 1, and an improvement of about 6 dB at $fT_b = 0.4$ is achieved for $m = 0.65$.

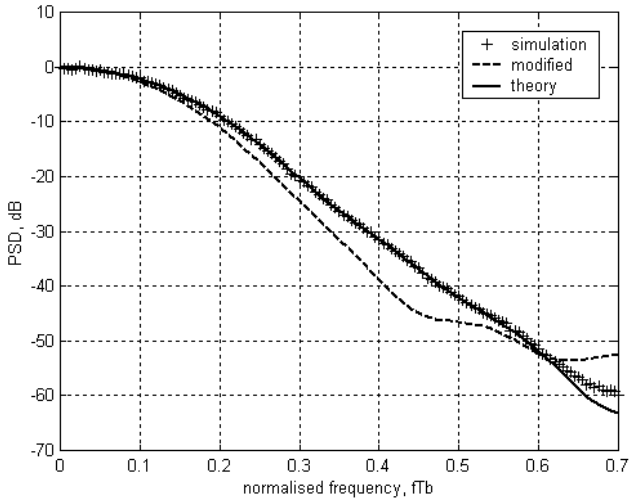


Fig. 1 Theoretical and simulated PSD for $M = 4$, 3RC, $h = 1/4$, and the theoretical PSD for a modified 3RC function

*B. Multi-h*

The gain relative to MSK can be expressed as

$$G_{MSK} = 10\log(d_{\min}^2/2)\ \text{dB} \qquad (7)$$

and for a BER of $10^{-6}$, MSK requires $E_b/N_0 \approx 10.5$ dB. For $M = 4$, 3RC, $h = 0.25$, a tight upper bound is $d_B^2 = 0.97$, giving $G_{MSK} = -3.2$ dB i.e. $E_b/N_0 \approx 13.8$ dB. This is shown as case A in Table 1, and falls outside the 12 dB specification. Rows B to J in the table show gains for some multi-*h* cases. Clearly, in order to obtain $\bar{h} \approx 0.25$, and so maintain an acceptable PSD, there should be at least 32 phase states (this is also the number of states used in [4]). Comparing $p = 32$ schemes, case H appears to have a power advantage of nearly 1.8 dB. However, it is shown in [5] that, for the same bandwidth efficiency and most practical $h$ values, $M = 8$ systems have inferior power gain when compared to the $M = 4$ systems. Case G offers about 2.8 dB advantage over case E, and 2.1 dB over case A, but at greatly increased complexity. The use of $p = 32$ and 3-cycle multi-*h* (3 *h* values) at best matched case F, i.e. a 4-fold increase in states gives just 1.2 dB gain over case A. Clearly, on this analysis, multi-*h* appears to offer little advantage over fixed *h*, and FEC is required in order to meet the 12 dB specification.

| | $M$ | $p$ | $S$ | $h_1$ | $h_2$ | $\bar{h}$ | $d_B^2$ | $G_{MSK}(dB)$ |
|---|---|---|---|---|---|---|---|---|
| A | 4 | 8 | 128 | 1/4 | 1/4 | 0.25 | 0.97 | - 3.2 |
| B | 4 | 8 | 128 | 1/4 | 1/2 | 0.375 | 1.93 | -0.15 |
| C | 4 | 16 | 256 | 1/4 | 3/8 | 0.3125 | 1.63 | - 0.89 |
| D | 4 | 16 | 256 | 1/8 | 1/4 | 0.1875 | 0.50 | - 6.02 |
| E | 4 | 32 | 512 | 3/16 | 5/16 | 0.25 | 0.81 | - 3.93 |
| F | 4 | 64 | 1024 | 7/32 | 9/32 | 0.25 | 1.26 | - 2.01 |
| G | 4 | 128 | 2048 | 15/64 | 17/64 | 0.25 | 1.55 | - 1.11 |
| H | 8 | 32 | 2048 | 3/16 | 5/16 | 0.25 | 1.21 | -2.18 |
| I | 8 | 64 | 4096 | 7/32 | 9/32 | 0.25 | 1.89 | -0.24 |
| J | 8 | 128 | 8192 | 15/64 | 17/64 | 0.25 | 2.33 | +0.66 |

Table 1. Gain relative to MSK for multi-*h* 3RC schemes

## III. NOISE MODELING

For simulation it is necessary to determine the rms noise $s_n$ corresponding to a specified $E_b/N_0$, and several methods are suggested in [6]. Here we adopt a relatively simple approach with the help of Fig. 2. Additive white noise is added to the CPM signal

$$s(t) = \sqrt{\frac{2E_s}{T_s}}\cdot\cos\left(w_c t + f(t,\underline{a}_n)\right) \qquad (8)$$

and is passed through an ideal bandpass filter of bandwidth *B*. The filter is assumed to have negligible effect upon the CPM spectrum, whilst permitting bandpass white noise of variance

$s_n^2 = N_0 B$ to be modeled as

$$n(t) = x_n(t)\cos w_c t - y_n(t)\sin w_c t \qquad (9)$$

Here $x_n(t)$ and $y_n(t)$ are statistically independent (and therefore uncorrelated) and each is drawn from a Gaussian process of variance $s_n^2$. Similarly, if the ideal lowpass filters of bandwidth $F$ do not significantly affect the signal, the complex envelope components over symbol period $nT \le t < (n+1)T$ are

$$\hat{I}(t) = I(t) + x_n(t) \quad ; \quad \hat{Q}(t) = Q(t) + y_n(t) \qquad (10)$$

where, for example, $I(t) = \sqrt{2E_s/T_s} \cdot \cos f(t, \underline{a}_n)$.

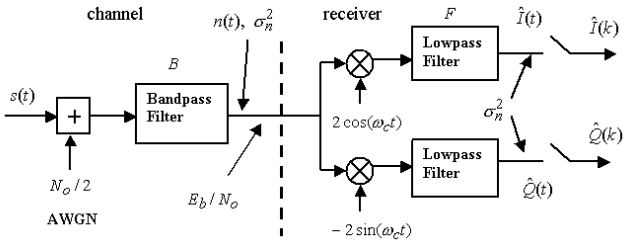


Fig. 2 Assumed noise model for *M*CPM

Signals $\hat{I}(t)$ and $\hat{Q}(t)$ are now over-sampled in order to perform a discrete approximation to matched filtering. The matched filters (not shown) generate the branch metric for Viterbi decoding. For example, assuming $m$ samples/symbol, the matched filter output for the $I$ component is

$$\hat{I}_{MF} = \sum_{k=0}^{m-1} \hat{I}(k) \cdot I_i(k) \;\; ; \;\; i = 1, 2, \ldots, pM^L \qquad (11)$$

where $I_i(k) = A\cos f_i(k, \underline{a}_n)$ is a possible transmitted signal, and $\hat{I}(k) = I(k) + x_n(k)$. The significant point is that $x_n(k)$ is an independent Gaussian noise sample of variance $s_n^2$. Independent noise samples are valid provided the filter output is sampled at the Nyquist rate, i.e. the filter bandwidth is assumed to be

$$F = \frac{B}{2} = \frac{m}{2T_s} = \frac{m}{2T_b \log_2 M} \qquad (12)$$

If the model samples $I$ and $Q$ components of amplitude $A = \sqrt{2E_s/T_s}$, the signal to noise ratio is

$$\frac{A^2/2}{s_n^2} = \frac{E_s/T_s}{N_0 B} \qquad (13)$$

Letting $A = 1$ and $E_s = E_b \log_2 M$,

$$s_n = \sqrt{\frac{m}{2 \cdot \log_2 M \cdot E_b/N_0}} \qquad (14)$$

The model assumes that the normalized lowpass filter bandwidth, $FT_b$, is high enough to avoid significant attenuation of the wideband CPM signal. For most cases of interest this is not a significant problem. As an example, for *L*RC schemes ($L > 1$) the PSD is typically -80 dB at $fT_b = 2$, and so $m \ge 8$ should more than suffice. Simpler CPM schemes have a broader main lobe e.g. the 8CPFSK $h = 1/4$ scheme described below is only 34 dB down at $fT_b = 1$, although this appears to be adequate. A loose upper bound on *m* is defined by the dimensionality theorem (section IV). Assuming the CPM signal is received according to the model in Fig. 2 i.e. it is a wideband signal, it is therefore valid to simulate it according to (14) using independent Gaussian noise samples. The wideband simulation can be directly compared to the standard matched filter bit error rate (BER) curve for MSK/QPSK.

### *A. 8CPFSK Simulation*

The noise model in (14) has been verified by BER simulation of Viterbi (i.e. matched filter) decoded 8CPFSK ($M = 8$) $h = 1/4$, Fig.3. Simulation is in very close agreement with an independent Viterbi decoder simulation of the same system [6], and with theoretical BER computation. For high $E_b/N_0$, the BER is approximated by

$$P_b \approx Q\left(\sqrt{d_B^2 \cdot E_b/N_0}\right) \;\; ; \;\; d_B^2 = 2.18 \qquad (15)$$

According to (7) the asymptotic gain relative to MSK should be about 0.4 dB. Simulation appears to be marginally more accurate for $m > 4$, and the larger values of *m* are expected to be needed for smoother phase responses. Note that there is redundancy in the maximum possible set of $pM^L$ complex signals defined in (11), and only $M^L$ complex matched filters are actually required [6].

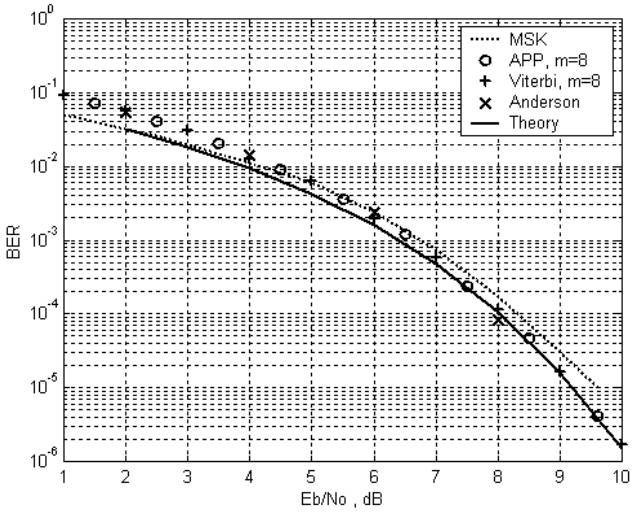


Fig. 3 BER simulation for 8CPFSK, $h = 1/4$ (APP decoding, Viterbi decoding, and theory)

## IV. APP DECODING OF CPM

APP decoding of CPM is needed to provide the soft output to an FEC decoder in coded CPM systems. The APP algorithm is well known [7] and here we simply highlight an implementation problem in the context of CPM.

Consider the decoding of data symbol $a$ over symbol period $nT \le t < (n+1)T$ given a received block of $N$ symbols $\mathbf{r}_1^N$. For this symbol period let the received baseband signal be $\mathbf{r}$. The APP decoder will decode $a$ as

$$P(a = k \mid \mathbf{r}_1^N) = \sum_{S_n, S_{n+1}} P(\mathbf{r} \mid \mathbf{s}_i) P(S_n = p) P_b(S_{n+1} = q) \qquad (16)$$

Here, summation is over all possible signals $\mathbf{s}_i$ and states $S_n, S_{n+1}$ corresponding to data $a = k$, and the last two probabilities are obtained from forward and backward recursions respectively. In [8], $P(\mathbf{r} \mid \mathbf{s}_i)$ is computed on a vector $\mathbf{r}$ corresponding to the outputs of a reduced set of $K < M^L$ complex matched filters.

An approximation to matched filtering is obtained by adopting an orthonormal expansion of the received baseband signal, $r(t)$. The general objective is to utilize a reduced signal space and so simplify the receiver. Using an orthogonal basis $\{y_j(t)\}$ defined over a specific time interval, a scalar signal $r(t)$ can be approximated over the same interval by

$$r(t) \approx \sum_{j=0}^{K-1} r_j y_j(t) \qquad (17)$$

where $r_j$ are coefficients of the expansion and $K$ is the signal space dimension. If $r(t) = s_i(t) + n(t)$, where $s_i(t)$ is a possible transmitted signal and $n(t)$ is a noise component, it follows that $r_j = s_{i,j} + n_j$, where $s_i(t)$ and $n(t)$ have been expanded as in (17). If $n(t)$ is Gaussian, it also follows from linearity that coefficients $r_j$ are Gaussian. Letting $\mathbf{r} = (r_0, r_1, \ldots, r_{K-1})$, $\mathbf{s}_i = (s_{i,0}, s_{i,1}, \ldots, s_{i,K-1})$, the Maximum Likelihood (ML) receiver will then select $s_i(t)$ (a long sequence of symbols) to maximize

$$p(\mathbf{r} \mid \mathbf{s}_i) = \left( \frac{1}{s_n \sqrt{2p}} \right)^K \cdot \exp\left[ - \frac{\sum_j (r_j - s_{i,j})^2}{2 s_n^2} \right] \qquad (18)$$

where $s_n^2$ is the variance of $r_j$. Now assume that $r(t)$ is the output from an ideal lowpass filter. If this is over-sampled at rate $m / T_s$ to give vector $\mathbf{r} = (r_0, r_1, ..., r_{m-1})$, then $r(t)$ can be expanded as in (17) over $nT_s \le t < (n+1)T_s$ with basis set

$$y_k(t) = \left\{ \frac{\sin\left[ \frac{p m}{T_s} \left( t - (n + \frac{k}{m}) T_s \right) \right]}{\frac{p m}{T_s} \left( t - (n + \frac{k}{m}) T_s \right)} \right\} \qquad (19)$$

This would tend to a complete set as $m$ becomes large. Given a set of quantized samples, (18) can be expressed over one symbol as

$$P(\mathbf{r} \mid \mathbf{s}_i) = \exp\left[ - \frac{\sum_{k=0}^{m-1} (r_k - s_{i,k})^2}{2 s_n^2} \right] \qquad (20)$$

Extension of (20) to the sampled complex baseband signal in Fig.2 is then straightforward. Let

$$\mathbf{r} = (\hat{\mathbf{I}}, \hat{\mathbf{Q}}) \;;\; \hat{\mathbf{I}} = [\hat{I}(0), \hat{I}(1), \ldots, \hat{I}(m-1)] \qquad (21)$$

The required probability conditioned on signal $\mathbf{s}_i = (\mathbf{I}_i, \mathbf{Q}_i)$ is the joint probability

$$P(\mathbf{r} \mid \mathbf{s}_i) = P(\hat{\mathbf{I}}, \hat{\mathbf{Q}} \mid \mathbf{I}_i, \mathbf{Q}_i) \qquad (22)$$

If $\hat{\mathbf{I}}$ and $\hat{\mathbf{Q}}$ are independent,

$$P(\mathbf{r} \mid \mathbf{s}_i) = P(\hat{\mathbf{I}} \mid \mathbf{I}_i) \cdot P(\hat{\mathbf{Q}} \mid \mathbf{Q}_i) \qquad (23)$$

$$= \exp\left[ - \frac{\left| \hat{\mathbf{I}} - \mathbf{I}_i \right|^2 + \left| \hat{\mathbf{Q}} - \mathbf{Q}_i \right|^2}{2 s_n^2} \right] \qquad (24)$$

$$= \exp\left[ - \frac{\sum_{k=0}^{m-1} \left\{ \left( \hat{I}(k) - I_i(k) \right)^2 + \left( \hat{Q}(k) - Q_i(k) \right)^2 \right\}}{2 s_n^2} \right] \qquad (25)$$

The squared Euclidean distances in (25) could be used as branch metrics in a Viterbi decoder. Alternatively, (25) can be used as the symbol transition probability in an APP decoder. Both systems approximate to ML decoding as $m$ increases. Put another way, over-sampling the lowpass filter outputs and APP decoding approximates to optimal decoding and no matched filtering is required.

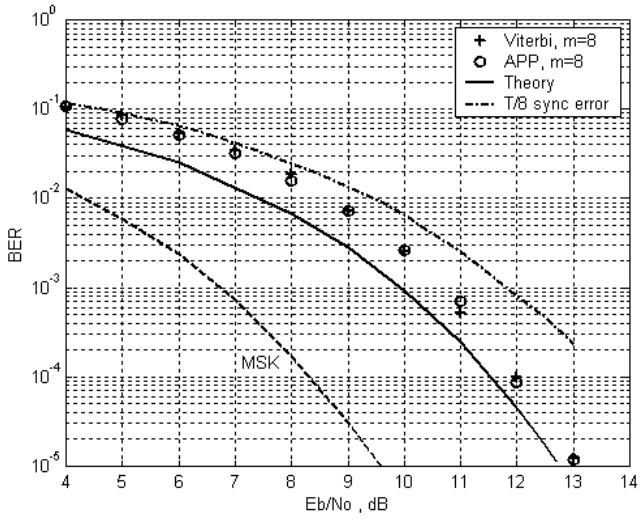


Fig. 4 BER simulation for quaternary 3RC $h = 1/4$

Some justification for writing (22) as (23) can be obtained from statistical tests, such as a hypothesis test in the form of a Likelihood Ratio based on the noisy $\hat{\mathbf{I}}$ and $\hat{\mathbf{Q}}$ signals. This test showed that for additive white Gaussian noise (AWGN) of standard deviation $s_n$, $\hat{\mathbf{I}}$ and $\hat{\mathbf{Q}}$ can be regarded as being

substantially independent when $s_n \geq 1, m = 4$ and $s_n \geq 1.5, m = 8$. It turns out that, for the values of $s_n$ computed in section III, this is quite a reasonable assumption, especially at the lower values of $E_b / N_0$.

### A. Walsh Signal Space

The over-sampled lowpass filter model in Fig.2 is convenient for simulation, but in practice it requires linear phase filters to avoid phase distortion of the CPM signal. This can be avoided by using Walsh [10] rather than sinc functions in (17). For example, using $K = 4$ dimensional Walsh space,

$$r_3 = \int_0^{T_S/4} r(t)dt - \int_{T_S/4}^{T_S/2} r(t)dt + \int_{T_S/2}^{3T_S/4} r(t)dt - \int_{3T_S/4}^{T_S} r(t)dt \qquad (21)$$

Coefficients $r_0, r_1, r_2$ are then easily computed from the four integrals in (21). The linear phase filters in Fig.2 are now replaced by simple integrators whose outputs are over-sampled by a factor *K*. For simulation purposes we assume $r(t)$ is over-sampled at rate $m / T_s$, giving samples $r_k$ with noise variance $s_n^2$, as in (14). For sufficiently large *m*, coefficient $r_j$ can then be estimated as

$$r_j \approx \frac{T_s}{m} \sum_{k=0}^{m-1} r_k \cdot w_{j,k} \quad ; \quad w_{j,k} \in \{\pm 1\} \qquad (22)$$

where $w_{j,k}$ is a sample of the *j*th Walsh function. Assuming quantized coefficients, the corresponding conditional probability for APP decoding is

$$P(\mathbf{r} \mid \mathbf{s}_i) = \exp\left[ - \frac{\sum_j \left(r_j - s_{i,j}\right)^2}{2 s_w^2} \right] \qquad (23)$$

where

$$s_w^2 = \frac{s_n^2}{m} = [\, 2 \log_2 M \cdot E_b / N_0 \,]^{-1} \qquad (24)$$

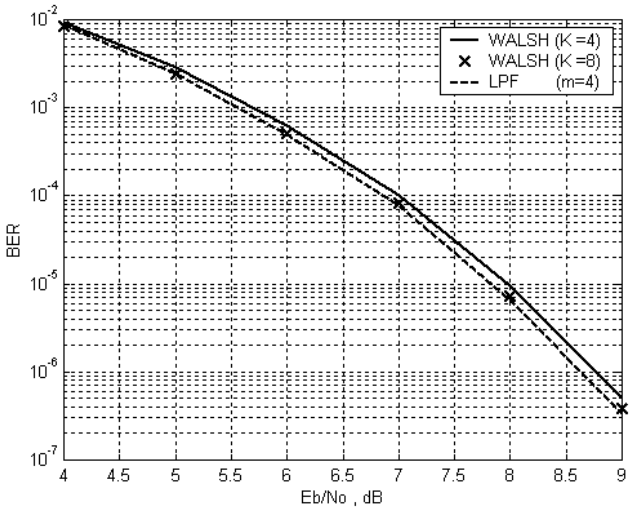


Fig. 5 BER simulation for quaternary 3RC $h = 1/2$

### B. Simulation

Fig. 3 shows simulation of APP-decoded 8CPFSK based upon (14) and (25). There is very close agreement with the two matched filter (Viterbi) simulations (as expected) and with theory. Fig. 4 compares a Viterbi simulation with simulated APP decoding for the quaternary 3RC $h = 1/4$ CPM system discussed in section II. Again, the two simulations are identical and are within 0.5 dB of theory for high $E_b / N_0$. Fig. 4 also shows the effect of a $T_s / 8$ symbol timing error.

The inherent assumption is that filtering does not affect the CPM signal i.e. no intersymbol interference is generated (in contrast to [9]). This being the case, the signal set defined in (11) applies. As stated, in practice, the in-band phase response of the lowpass filter can adversely affect the CPM signal and so phase linearity is important.

Fig. 5 shows Walsh and lowpass filter simulations for a quaternary 3RC $h = 0.5$ system. The discrepancy of approximately 0.1 dB for an over-sampling factor of 4 is attributed to the fact that CPM signals are comparatively poorly represented in Walsh space. The degree of over-sampling is governed by the dimensionality theorem, which indicates that *m* or *K* need only be a small integer for most CPM signals. In particular, BER simulations for $m = 4$ show no significant difference to those for $m = 8$.

## V. CODED CPM

Rimoldi [11] showed that *M*CPM can be decomposed into a continuous phase recursive encoder (CPE) and a memoryless modulator/mapper (MM). The CPE can therefore provide the inner code of a serial concatenated convolutional code (SCCC) [12]. This structure is attractive, given new high rate convolutional codes for the outer code [13]. The authors are currently investigating the use of such codes for SCCC-CPM.

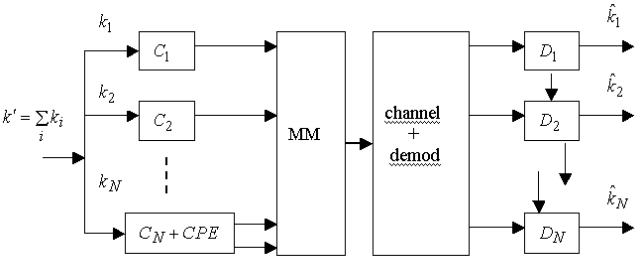


Fig. 6 Multilevel coded CPM using multistage binary decoding.

Whilst SCCC-CPM systems have high potential, they do not deliberately combine FEC with CPM in the coded modulation sense (there is no set partitioning). Two well-known approaches to Shannon capacity are trellis-coded modulation, and multilevel coding, and a multilevel coding scheme for CPM is shown in Fig. 6. *M*CPM has $PM^L = 2^J$ points in signal space, where $P = K / h$ (*K* integer) is the number of phase states in the time-invariant Rimoldi model. The usual approach

in multilevel coding would be to partition the information stream into $J$ binary substreams encoded by $J$ binary component codes, $C_i$. For CPM, set partitioning is constrained by the need to maintain phase continuity. For example, certain $M$CPFSK systems can have parallel phase transitions between the same phase states (corresponding to different frequency signals). In such cases, phase continuity can be achieved by assigning these signals to different subsets at the same level, and the number of levels would be $N = \log_2(2M/P)$. The decoder uses multistage soft decision decoding, whereby an estimate of the code sequence at level $j$ is fed to the decoder at level $j+1$.

Design rules for multilevel systems are centered on optimizing the code rate at each level e.g. codes $C_i$ are designed to maximize the overall minimum Euclidean distance in signal space. Given appropriate codes, the sum of the capacities at each level can then approach the capacity of the $2^N$-ary modulation scheme [14]. Powerful codes are assigned to the low levels e.g. $C_i$ could be a high rate binary SCCC, as in [13]. Alternatively we could use a binary turbo product code (TPC) based on extended Hamming codes e.g. the $(64,57)\times(64,57)$, $R = 0.793$ code [15]. For this code, APP decoding of the overall TPC is unrealistic, although it is feasible for the component codes. For the $(64,57)$ code the complexity is similar to that for decoding a memory-5 convolutional code. Only a relatively weak code is required at level $N$, which is combined with the CPE of the CPM system as indicated in Fig.6.

## VI. CONCLUSIONS

A realistic practical example has illustrated that CPM system design is a complex trade-off between the CPM parameters themselves and also between the CPM system and any external FEC. It is shown that multi-$h$ systems are not always beneficial due to the greatly increased number of states, and for low values of $h$ the required coding gain is probably better achieved via FEC. It is also shown that modification to the raised cosine frequency pulse can give significant improvement to the power density at important frequencies.

Simulation is an important aspect in CPM system design, and fast and accurate power density simulation is achieved using the classical periodogram technique. Simulation of APP-decoded CPM can use a simple probability measure based on $m$-times over-sampling of the outputs from ideal lowpass filters, or on $K$-times over-sampling of the integrators in a Walsh-based CPM system. The lowpass filter approach assumes that filtering does not significantly degrade the CPM signal. Both decoding techniques approximate to the ML decoder as the over-sampling factor increases, and can be viewed as greatly simplified matched filtering. Four-times over-sampling is found to be sufficient, and both APP and Viterbi simulations are generally within 0.5 dB of theory at high $E_b/N_0$.

The wideband signal model also permits straightforward computation of the noise variance required for BER simulation of APP decoded CPM. The noise model is adequate since most CPM signals have a compact power spectrum. Modeling assumptions are verified by comparison with independent simulation and with theory.

In terms of bandwidth and power efficiency, a near ideal but realistic modulation scheme could comprise a multilevel coded CPM system, with multistage binary decoding. Multilevel coded CPM can approach capacity with realistic decoding complexity. New, high rate binary convolutional codes in SCCC structures are particularly attractive for the lower levels.

## REFERENCES


[1] A. Svensson, "Reduced state sequence detection of partial response continuous phase modulation," *IEE Proc.*, vol. 138, no. 4, Aug. 1991, pp. 256-268.

[2] G. Colavolpe and R. Raheli, "Reduced-complexity detection and phase synchronization of CPM signals," *IEEE Trans. on Communications*, vol. 45, no. 9, Sept. 1997, pp. 1070-1079.

[3] J. Proakis, *Digital Communications, 3rd Ed.*, McGraw-Hill, 1995, pp. 209-219.

[4] Interoperability standard for single-access 5-kHz and 25-kHz UHF satellite communications channels: MIL-STD-188-181B, March 1999.

[5] C-E. Sundberg, "Continuous phase modulation," *IEEE Communications Mag.*, vol. 24, no.4, April 1986, pp. 25-38.

[6] J. Anderson, T. Aulin, and C-E Sundberg, "*Digital phase modulation*, " Plenum, New York, 1986, pp. 257-261.

[7] L. Bahl, J. Cocke, F. Jelinek, and J. Raviv, "Optimum decoding of linear codes for minimizing symbol error rate," *IEEE Trans. on Information Theory*, March 1974, pp. 284-287.

[8] P. Moqvist, "Serially concatenated systems: an iterative decoding approach with application to continuous phase modulation", *Thesis for the degree of Licentiate of Engineering*, Dept. of Computer Engineering, Chalmers University of Technology, Goteborg, Sweden, Nov. 1999.

[9] S. Simmons, "Simplified Coherent Detection of CPM", *IEEE Trans. on Communications*, vol. 43, no. 2/3/4 February/March/April, 1995, pp 726-728.

[10] W. Tang, and E. Shwedyk, "A Quasi-Optimum Receiver for Continuous Phase Modulation", *IEEE Trans. on Communications*, vol. 48. no.7, July 2000, pp. 1087-1090.

[11] B. Rimoldi, "A decomposition approach to CPM", *IEEE Trans. on Information Theory*, vol. 34, no.2, March 1988, pp 260-270.

[12] P. Moqvist and T. Aulin, "Serially concatenated continuous phase modulation with iterative decoding", *IEEE Trans. on* Communications, vol. 49, Nov. 2001, pp. 1901-1915.

[13] A. Amat, G. Montorsi, and S. Benedetto, "New High-rate Convolutional Codes for Concatenated Schemes", ICC'2002, April 28 - May 2, New York, 2002.

[14] U. Wachsmann, R. Fischer and J. Huber, "Multilevel Codes: Theoretical Concepts and Practical Design Rules", *IEEE Trans. on Information Theory*, vol. 45, no.5, July 1999, pp 1361-1391.

[15] M. Tomlinson, G. Wade, P. van Eetvelt, A. Ambroze, "Bounds for finite block-length codes", *IEE Proceedings – Communications*, vol. 149, no. 2, April 2002, pp. 65-69.